

Highly Efficient Cooperative Catalysis of Single-Site Lewis Acid and Brønsted Acid in a Metal–Organic Framework for the Biginelli Reaction

Si-Yu Zhao,[†] Zhi-Yan Chen,[†] Na Wei,[‡] Lin Liu,^{*,†,‡} and Zheng-Bo Han^{*,†,‡}

[†]College of Chemistry, Liaoning University, Shenyang 110036, P. R. China

[‡]Institute of Catalysis for Energy and Environment, College of Chemistry and Chemical Engineering, Shenyang Normal University, Shenyang 110034, P. R. China

S Supporting Information

ABSTRACT: A unique 3D framework containing three different types of nanoscale polyhedron cages was constructed by incorporating dinuclear $[M_2(\mu_2\text{-OH})(\text{COO})_4]$ ($M = \text{Co}, \text{Ni}$) secondary building units and pyridyl-carboxylic-acid-supported tetracarboxylates. The assembled complexes possess isolated bifunctional single-site Lewis acid and Brønsted acid and can be used as highly efficient heterogeneous catalysts for the solvent-free Biginelli reaction with a high turnover frequency value of 338.4 h^{-1} . Interestingly, a variety of 3,4-dihydropyrimidin-2(1H)-ones have been obtained in high yields and short times.

Single-site catalysts, as heterogeneous catalysts with isolated active sites, have gradually become the frontier research field in diverse reactions.¹ As reported, the single-site catalysts combine the excellent catalytic performance of homogeneous catalysts with the classical advantages of heterogeneous catalysts, which can be removed from the mixture reaction and recycled.² Furthermore, most catalysts have catalytic functions that are more complex and difficult to control, whereas single-site catalysts are relatively simple and easy.³ Therefore, single-site catalysts for catalyzing organic reactions are not only a green, cost-effective process but also maximize atomic utilization.⁴ Although great progress has been achieved, the fabrication of single-site catalysts with high density and uniform distribution of bifunctional active sites remains a significant challenge.⁵

Metal–organic frameworks (MOFs) are a highly versatile type of crystalline porous materials formed by metal centers and organic ligands,⁶ which have been widely used in gas storage and separation⁷ and catalysis.⁸ More importantly, their periodic network structure results in the spatial separation of unsaturated metal sites and functional organic ligands, which makes MOFs promising candidates for bifunctional single-site catalysts.⁹ As an example, Zhou and coworkers demonstrated PCN-124, which contains various functional groups and exhibits excellent catalytic activity in the tandem deacetalization–Knoevenagel condensation reaction.¹⁰ Recent reports have illustrated some examples where different approaches have been applied to create MOF bifunctional single-site catalysts.¹¹ One way is the use of postsynthesis modification,

which may cause the metal ion precursors to aggregate on the surface of MOFs and seriously block the pores. As a result, their catalytic behaviors will be limited due to the low diffusion efficiency of the substrates.¹² Another efficient way is to integrate the metal active sites as inorganic nodes with functional organic ligands by a rational design, which makes the bifunctional active sites in MOFs have a uniform dispersion.¹³ Hence, the design and synthesis of easily prepared, efficient, and bifunctional single-site MOF catalysts urgently require further development.

In this work, a unique 3D framework incorporating $[M_2(\mu_2\text{-OH})(\text{COO})_4]$ ($M = \text{Co}, \text{Ni}$) secondary building units (SBUs) (Figure 1a) and pyridyl-carboxylic-acid-supported tetracarboxylates was successfully synthesized by direct self-assembly methods with the formula $[(\text{CH}_3)_2\text{NH}_2][M_2(\mu_2\text{-OH})(\text{COO})_4(\text{HDDIA})(\text{H}_2\text{O})_2] \cdot (\text{solv})_x$ (M-DDIA), [$\text{H}_5\text{DDIA} = 2,5\text{-di}(3,5\text{-dicarboxyl-phenyl})\text{isonicotinic acid}$]. The resulting materials were expected to exhibit highly dispersed active sites with a uniform distribution of nanocages that might be more favorable for trapping substrate molecules. More strikingly, Ni-DDIA demonstrates a higher catalytic performance toward the Biginelli reaction under solvent-free conditions, surpassing almost all reported MOF-based catalysts due to the cooperative effect of the Lewis acidic Ni(II) sites and Brønsted acidic $-\text{COOH}$ groups.

The reaction of $M(\text{NO}_3)_2 \cdot 6\text{H}_2\text{O}$ ($M = \text{Co}$ and Ni) with H_5DDIA in a mixture of dimethylformamide (DMF) and H_2O at 85°C affords crystals of M-DDIA. Single-crystal X-ray crystallography showed that Co-DDIA crystallizes in the cubic space group $Fm\bar{3}m$ (Table S1)¹⁴ and exhibits a 3D porous structure with a high density of coordinatively unsaturated metal sites and uncoordinated carboxyl groups on the surfaces of the pores. In one asymmetric unit, there are two crystallographically independent Co^{2+} ions that form a dinuclear $\text{Co}_2(\mu_2\text{-OH})(\text{COO})_4$ (abbreviated as Co_2) cluster as an SBU (Figure 1a), one HDDIA^{4-} , two coordinated water molecules, one $\mu_2\text{-OH}$, and $1/4$ $[(\text{CH}_3)_2\text{NH}_2]^+$ originating from the decomposition of DMF during the reaction. The Co_2 cluster adopts a D_{4h} symmetry, alternately connected by four carboxylate groups of organic linkers and terminal H_2O moieties. Each H_5DDIA ligand is connected to four Co_2

Received: March 21, 2019

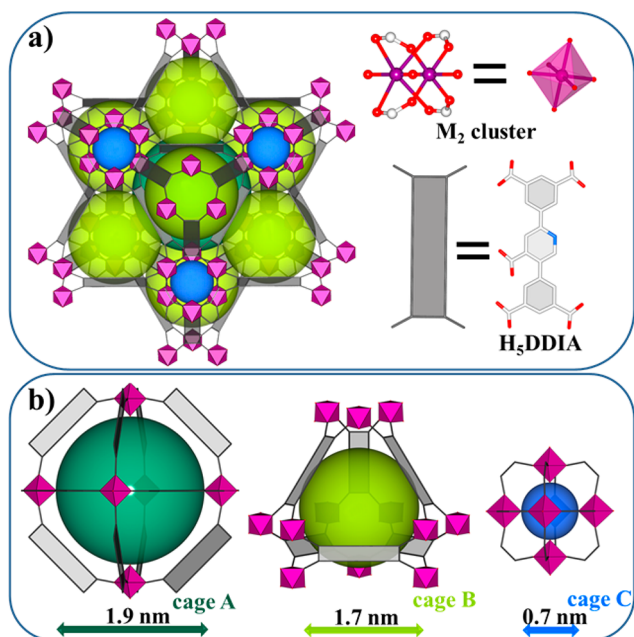


Figure 1. Single-crystal structure for M-DDIA: (a) Polyhedron view of the 3D frameworks. (b) Three types of cages: the large octahedron cage (left), medium tetrahedron cage (middle), and small hexahedron cage (right). Guest molecules, water molecules, and H atoms have been omitted for clarity. Color code: metal ions, purple; O, red; N, blue; C, gray.

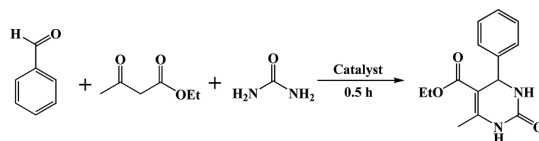
clusters, resulting in a 3D porous framework. Co-DDIA features three types of nanocages: a large $M_{12}L_{12}$ octahedron cage, which is composed of eight HDDIA⁴⁻ ligands with a cage diameter of 1.9 nm (Figure 1b, left); a medium $M_{24}L_6$ tetrahedron cage, which is composed of six HDDIA⁴⁻ ligands with a 1.7 nm diameter (Figure 1b, middle); and a small

octahedron that is also composed of 12 HDDIA⁴⁻ ligands with a cage diameter of 0.7 nm (Figure 1b, right). These three cages are in a staggered configuration (Figure 1a). The powder X-ray diffraction (PXRD) patterns demonstrate the isostructural nature of Co-DDIA and Ni-DDIA (Figure S1). The PLATON¹⁵ calculation certifies that the total solvent-accessible volume of Co-DDIA is 41254.6 Å³ per unit cell, which makes up ~61.4% of the cell volume. From the topological point of view, if the HDDIA⁴⁻ ligand and Co₂ cluster are considered as four-connected nodes, then the 3D structure of the Co-DDIA can be simplified as an NbO topology with a Schläfli symbol of 6⁴·8².¹⁶

To investigate the chemical stabilities of Co-DDIA and Ni-DDIA, the samples were soaked in dichloromethane, methylbenzene, acetonitrile, benzaldehyde, and ethylacetate for 24 h. The unaltered PXRD patterns indicated that the samples maintain the crystallinity after solvent treatment (Figures S2–S4). The thermal stability of the three MOFs was tested by thermal gravimetric analysis (TGA), revealing that the decomposition temperature is ~400 °C (Figure S5).

Recently, MOFs as single-site catalysts with high catalytic performance in organic reactions have attracted more concern of researchers. However, the precise fabrication of bifunctional single-site MOFs that catalyze multicomponent reactions has been rarely reported. For the multicomponent reactions, the Biginelli reaction has caused widespread concern because the products of this reaction are 3,4-dihydropyrimidin-2(1H)-ones (DHPMs) which are vital medicinal synthones having pharmacological and therapeutic properties such as antibacterial, calcium antagonism, antihypertension, α_{1a} -adrenoceptor-selective antagonism, and anticancer properties.¹⁷ Taking advantage of the high density of isolated Lewis and Brønsted acid sites, the excellent chemical stability, and the nanocages in the framework, we intend to explore the catalytic activity of Co-DDIA and Ni-DDIA for the Biginelli reaction to form

Table 1. One-Pot Multicomponent Biginelli Reaction^a



entry	catalyst (mmol)	solvent	T (K)	yield (%) ^b	TOF (h ⁻¹) ^c
1	Ni-DDIA (0.005)	none	353	84.6	338.4
2	Ni-DDIA (0.010)	none	353	90.4	180.8
3	Ni-DDIA (0.015)	none	353	96.1	128.1
4	Ni-DDIA (0.020)	none	353	90.0	90.0
5	Ni-DDIA (0.015)	none	333	87.7	117.4
6	Ni-DDIA (0.015)	none	343	93.4	124.6
7	Ni-DDIA (0.015)	none	363	96.0	128.0
8	Ni-DDIA (0.015)	DMF	353	70.0	93.4
9	Ni-DDIA (0.015)	CH ₃ CN	353	62.0	82.6
10	Ni-DDIA (0.015)	CH ₂ Cl ₂	313	40.0	53.4
11	Ni-DDIA (0.015)	toluene	353	53.0	70.6
12	Co-DDIA (0.015)	none	353	82.6	110.0
13	Ni(NO ₃) ₂ (0.015)	none	353	58.1	77.4
14	UiO-66 (0.015)	none	353	62.7	83.6
15	MIL-101 (0.015)	none	353	60.3	80.4
16	Ni-TPTC (0.015)	none	353	80.5	107.4

^aReaction conditions: benzaldehyde (1.0 mmol), ethylacetate (1.0 mmol), urea (1.5 mmol), 0.5 h, solvent (2.0 mL), under a N₂ atmosphere.

^bIsolated yield. The yields were monitored by TLC. ^cTOF: Moles of yielded product per mole of catalyst per hour.

DHPMs. To optimize the reaction conditions, a series of control experiments was conducted to study the influence of various parameters on this reaction, and the results are summarized in Table 1. Ni-DDIA could efficiently form 6-methyl-2-oxo-4-phenyl-1,2,3,4-tetrahydro-pyrimidine-5-carboxylic acid ethyl ester with a high yield of 96.1% and a remarkable turnover frequency (TOF) value of 128.1 h^{-1} under a relatively mild condition (353 K) for 0.5 h (Table 1, entry 3). At 0.005 mmol Ni-DDIA, the reaction proceeded to give the product in 84.6% yield, leading to a high TOF of 338.4 h^{-1} (entry 1). Its catalytic performance surpasses that of many reported MOFs under similar conditions, such as PTA@MIL-101,¹⁸ Cu-MOF,¹⁹ IRMOF-3,²⁰ Zn-MOF,²¹ $[\text{Co}(\text{DPP})_2(\text{H}_2\text{O})_2] \cdot (\text{BS})_2 \cdot 2\text{H}_2\text{O}$,²² and $\text{TiCl}_4\text{-MgCl}_2 \cdot 4\text{CH}_3\text{OH}$ ²³ (Table S2). Then, we intensively surveyed the influence of organic solvents on the catalytic system. Various solvents were introduced into the Biginelli reaction, such as DMF, CH_3CN , toluene, and CH_2Cl_2 (Table 1, entries 8–11). The reaction yield under solvent-free conditions was higher in comparison with solvent conditions, and the reaction time was also significantly shortened. The diversity of catalytic capacities between Ni-DDIA and Co-DDIA (82.6%, Table 1, entry 12) may contribute to the different atomic radii ($\text{Ni} < \text{Co}$). Furthermore, Ni-DDIA outperforms the benchmark cage-containing MOFs, UiO-66 and MIL-101, which exhibit moderate activities with yields of 62.7 and 60.3%, respectively, under the same conditions (Table 1, entries 14 and 15).

To explore the catalytic mechanism for the Biginelli reaction of Ni-DDIA, Ni-TPTC ($\text{H}_4\text{TPTC} = (1,1':4',1''\text{-terphenyl})\text{-}3,3',5,5''\text{-tetracarboxylic acid}$) without Brønsted acid sites was constructed. The PXRD pattern demonstrated the isostructural nature of Ni-DDIA and Ni-TPTC (Figure S1). While maintaining the amount of catalyst and other conditions, the yield of 6-methyl-2-oxo-4-phenyl-1,2,3,4-tetrahydro-pyrimidine-5-carboxylic acid ethyl ester was 80.5% after 0.5 h with Ni-TPTC (Table 1, entry 16). This finding further demonstrates that the uncoordinated $-\text{COOH}$ groups in Ni-DDIA act as a Brønsted acid having a cooperative effect with the Lewis acidic Ni(II) sites, further enhancing the catalytic performance. Moreover, the Py-IR spectra of Ni-DDIA and Ni-TPTC confirm this conjecture (Figure S6). The concentrations of Lewis and Brønsted acidic sites in Ni-DDIA are 0.0114 and 0.0173 mmol/g, respectively, which have been estimated by integrating the peaks at 1448 and 1531 cm^{-1} . The concentration of Lewis acidic sites in Ni-TPTC is 0.0010 mmol/g.²⁴ On the basis of the above catalysis results and structural analysis, a possible cooperative catalytic mechanism for Biginelli reaction is proposed. As illustrated in Figure 2, the *N*-acylimine intermediate formation from aldehyde and urea is owing to the existence of Lewis acidic Ni(II) sites and Brønsted acidic $-\text{COOH}$ sites. Then, the enol tautomer of ethyl acetoacetate reacts with *N*-acylimine intermediate to form ureide. The final step of the reaction is the cyclodehydration of ureide under acid catalysis to form the corresponding DHPM products. Here Ni-DDIA has a large number of dispersed Brønsted acidic $-\text{COOH}$ groups and Lewis acidic Ni(II) centers, which gives excellent catalytic performance to the reaction.

With the optimized conditions (no solvent, 353 K), several typical aromatic aldehyde substrates were subjected to this Biginelli reaction (Table S3). The products were determined by ^1H NMR (Figures S7–S12). Under the standard conditions, the corresponding products were obtained in

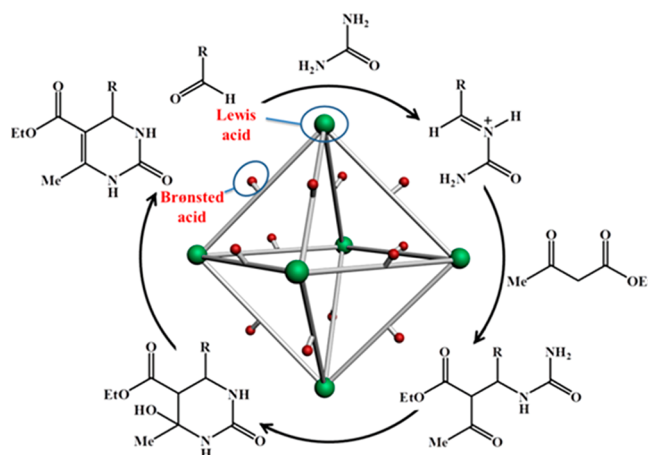


Figure 2. Proposed reaction mechanism for the Biginelli reaction catalyzed by Ni-DDIA.

excellent yields. After 0.5 h, Ni-DDIA (0.015 mmol) afforded high yields of 4-(4-fluorophenyl)-6-methyl-2-oxo-1,2,3,4-tetrahydro-pyrimidine-5-carboxylic acid ethyl ester (88.3%, Table S3, entry 1), 4-(4-chlorophenyl)-6-methyl-2-oxo-1,2,3,4-tetrahydro-pyrimidine-5-carboxylic acid ethyl ester (89%, Table S3, entry 2), 4-(4-bromophenyl)-6-methyl-2-oxo-1,2,3,4-tetrahydro-pyrimidine-5-carboxylic acid ethyl ester (90%, Table S3, entry 3), 6-methyl-2-oxo-4-*p*-tolyl-1,2,3,4-tetrahydro-pyrimidine-5-carboxylic acid ethyl ester (92%, Table S3, entry 4), and 4-(4-methoxy-phenyl)-6-methyl-2-oxo-1,2,3,4-tetrahydro-pyrimidine-5-carboxylic acid ethyl ester (93.2%, Table S3, entry 5).

After the end of the reaction, catalyst Ni-DDIA is separated by filtration and passed through multiple parallel experiments to obtain a sufficient catalyst for the next cycle. After five runs of the reaction, the yield can still reach >90%, and there is no significant change in the TON values (Figure S13), indicating that the catalytic performance of the catalyst is not attenuated during the continuous five runs of catalysis. The PXRD pattern from the recovered catalyst was identical to the as-synthesized one, which confirms the stability of the Ni-DDIA catalyst during the reactions (Figure S14).

In summary, we have successfully synthesized dinuclear $\text{Co}^{2+}/\text{Ni}^{2+}$ -based MOFs, M-DDIA ($M = \text{Co}$ and Ni), with unique 3D frameworks containing three different types of nanoscale polyhedron cages. These constructed MOFs possess a high density of isolated bifunctional Lewis acid and Brønsted acid sites, which can serve as potential heterogeneous catalysts for the Biginelli reaction. The nondeactivation behavior and good recyclability of the present catalytic process verify the robustness and practical applicability of the MOFs as sustainable single-site catalysts. Introducing functional $-\text{COOH}$ groups into the framework during the assembly process enhances the catalytic activity of Ni-DDIA owing to the cooperative behavior of Lewis acidic Ni(II) sites and Brønsted acidic $-\text{COOH}$ groups. Ni-DDIA is an efficient bifunctional catalyst and is expected to be used in various reactions, such as the cyanosilylation reaction, the Strecker reaction, Diels–Alder reactions, the Prins reaction, and so on. Our further investigation is to design and synthesize bifunctional single-site MOFs heterogeneous catalysts for the efficient catalysis of multicomponent reactions.

■ ASSOCIATED CONTENT

Supporting Information

The Supporting Information is available free of charge on the ACS Publications website at DOI: 10.1021/acs.inorgchem.9b00816.

Experimental and synthesis procedures, physical characterization data, and details of catalysis (PDF)

Accession Codes

CCDC 1890658 contains the supplementary crystallographic data for this paper. These data can be obtained free of charge via www.ccdc.cam.ac.uk/data_request/cif, or by emailing data_request@ccdc.cam.ac.uk, or by contacting The Cambridge Crystallographic Data Centre, 12 Union Road, Cambridge CB2 1EZ, UK; fax: +44 1223 336033.

■ AUTHOR INFORMATION

Corresponding Authors

*L.L.: E-mail: liulin@lnu.edu.cn.

*Z.-B.H.: E-mail: ceshzb@lnu.edu.cn.

ORCID

Lin Liu: 0000-0002-9164-1190

Zheng-Bo Han: 0000-0001-8635-9783

Notes

The authors declare no competing financial interest.

■ ACKNOWLEDGMENTS

We thank the National Natural Science Foundation of China (21701076 and 21671090), LiaoNing Revitalization Talents Program (XLYC1802125), and Liaoning Province Doctor Startup Fund (20180540056) for financial support of this work.

■ REFERENCES

- (1) (a) Manna, K.; Ji, P. F.; Greene, F. X.; Lin, W. B. Metal–Organic Framework Nodes Support Single-Site Magnesium–Alkyl Catalysts for Hydroboration and Hydroamination Reactions. *J. Am. Chem. Soc.* **2016**, *138*, 7488–7491. (b) Manna, K.; Ji, P. F.; Lin, Z. K.; Greene, F. X.; Urban, A.; Thacker, N. C.; Lin, W. B. Chemoselective single-site Earth-abundant metal catalysts at metal–organic framework nodes. *Nat. Commun.* **2016**, *7*, 12610–12620. (c) Babucci, M.; Fang, C.-Y.; Perez-Aguilar, J. E.; Hoffman, A. S.; Boubnov, A.; Guan, E.; Bare, S. R.; Gates, B. C.; Uzun, A. Controlling catalytic activity and selectivity for partial hydrogenation by tuning the environment around active sites in iridium complexes bonded to supports. *Chem. Sci.* **2019**, *10*, 2623–2632.
- (2) (a) Genna, D. T.; Wong-Foy, A. G.; Matzger, A. J.; Sanford, M. S. Heterogenization of Homogeneous Catalysts in Metal–Organic Frameworks via Cation Exchange. *J. Am. Chem. Soc.* **2013**, *135*, 10586–10589. (b) Gong, L. L.; Feng, X. F.; Luo, F.; Yi, X. F.; Zheng, A. M. Removal and safe reuse of highly toxic allyl alcohol using a highly selective photo-sensitive metal–organic framework. *Green Chem.* **2016**, *18*, 2047–2055.
- (3) (a) Comito, R. J.; Wu, Z. W.; Zhang, G. H.; Lawrence, J. A.; Korzynski, M. D.; Kehl, J. A.; Miller, J. T.; Dinca, M. Stabilized Vanadium Catalyst for Olefin Polymerization by Site Isolation in a Metal–Organic Framework. *Angew. Chem., Int. Ed.* **2018**, *57*, 8135–8139. (b) Dubey, R. J. C.; Comito, R. J.; Wu, Z. W.; Zhang, G. H.; Rieth, A. J.; Hendon, C. H.; Miller, J. T.; Dinca, M. Highly Stereoselective Heterogeneous Diene Polymerization by CoMFU-4l: A Single-Site Catalyst Prepared by Cation Exchange. *J. Am. Chem. Soc.* **2017**, *139*, 12664–12669.
- (4) (a) Zhu, C. Z.; Fu, S. F.; Shi, Q. R.; Du, D.; Lin, Y. H. Single-Atom Electrocatalysts. *Angew. Chem., Int. Ed.* **2017**, *56*, 13944–13960. (b) Jiao, J.; Lin, R.; Liu, S.; Cheong, W.-C.; Zhang, C.; Chen, Z.; Pan,

Y.; Tang, J.; Wu, K.; Hung, S.-F.; Chen, H. M.; Zheng, L.; Lu, Q.; Yang, X.; Xu, B.; Xiao, H.; Li, J.; Wang, D.; Peng, Q.; Chen, C.; Li, Y. Copper atom-pair catalyst anchored on alloy nanowires for selective and efficient electrochemical reduction of CO₂. *Nat. Chem.* **2019**, *11*, 222–228.

(5) Canivet, J.; Aguado, S.; Schuurman, Y.; Farrusseng, D. MOF-Supported Selective Ethylene Dimerization Single-Site Catalysts through One-Pot Postsynthetic Modification. *J. Am. Chem. Soc.* **2013**, *135*, 4195–4198.

(6) (a) Yang, D.; Momeni, M. R.; Demir, H.; Pahls, D. R.; Rimoldi, M.; Wang, T. C.; Farha, O. K.; Hupp, J. T.; Cramer, C. J.; Gates, B. C.; Gagliardi, L. Tuning the properties of metal–organic framework nodes as supports of single-site iridium catalysts: node modification by atomic layer deposition of aluminium. *Faraday Discuss.* **2017**, *201*, 195–206. (b) Cao, L. Y.; Lin, Z. K.; Peng, F.; Wang, W. W.; Huang, R. Y.; Wang, C.; Yan, J. W.; Liang, J.; Zhang, Z. M.; Zhang, T.; Long, L. S.; Sun, J. L.; Lin, W. B. Self-Supporting Metal–Organic Layers as Single-Site Solid Catalysts. *Angew. Chem.* **2016**, *128*, 5046–5050.

(7) Alezi, D.; Belmabkhout, Y.; Suyetin, M.; Bhatt, P. M.; Weselinski, E.; Solovyeva, J.; Adil, V. K.; Spanopoulos, I.; Trikalitis, P. N.; Emwas, A.-H.; Eddaoudi, M. MOF Crystal Chemistry Paving the Way to Gas Storage Needs: Aluminum-Based soc-MOF for CH₄, O₂, and CO₂ Storage. *J. Am. Chem. Soc.* **2015**, *137*, 13308–13318.

(8) (a) Huang, Y. B.; Liang, J.; Wang, X. S.; Cao, R. Multifunctional metal–organic framework catalysts: synergistic catalysis and tandem reactions. *Chem. Soc. Rev.* **2017**, *46*, 126–157. (b) Wei, N.; Zuo, R. X.; Zhang, Y. Y.; Han, Z. B.; Gu, X. J. Robust high-connected rare-earth MOFs as efficient heterogeneous catalysts for CO₂ conversion. *Chem. Commun.* **2017**, *53*, 3224–3227. (c) Zhang, Y.; Wang, Y. X.; Liu, L.; Wei, N.; Gao, M. L.; Zhao, D.; Han, Z. B. Robust Bifunctional Lanthanide Cluster Based Metal–Organic Frameworks (MOFs) for Tandem Deacetalization–Knoevenagel Reaction. *Inorg. Chem.* **2018**, *57*, 2193–2198.

(9) (a) Yuan, J.; Fracaroli, A. M.; Klemperer, W. G. Convergent Synthesis of a Metal–Organic Framework Supported Olefin Metathesis Catalyst. *Organometallics* **2016**, *35*, 2149–2155. (b) Ye, J. Y.; Gagliardi, L.; Cramer, C. J.; Truhlar, D. G. Computational screening of MOF-supported transition metal catalysts for activity and selectivity in ethylene dimerization. *J. Catal.* **2018**, *360*, 160–167.

(10) Park, J.; Li, J. R.; Chen, Y. P.; Yu, J.; Yakovenko, A. A.; Wang, Z. U.; Sun, L. B.; Balbuena, P. B.; Zhou, H.-C. A versatile metal–organic framework for carbon dioxide capture and cooperative catalysis. *Chem. Commun.* **2012**, *48*, 9995–9997.

(11) (a) Abdel-Mageed, A. M.; Rungtaweeworanit, B.; Parlinska-Wojtan, M.; Pei, X.; Yaghi, O. M.; Behm, R. J. Highly Active and Stable Single-Atom Cu Catalysts Supported by a Metal–Organic Framework. *J. Am. Chem. Soc.* **2019**, *141*, 5201. (b) Hossain, S.; Jin, M. J.; Park, J.; Yingjie, Q.; Yang, D. A. Oxidation and Reduction of Various Substrates Over a Pd(II) Containing Post-Synthesis Metal Organic Framework. *Catal. Lett.* **2013**, *143*, 122–125.

(12) Canivet, J.; Aguado, S.; Schuurman, Y.; Farrusseng, D. MOF-Supported Selective Ethylene Dimerization Single-Site Catalysts through One-Pot Postsynthetic Modification. *J. Am. Chem. Soc.* **2013**, *135*, 4195–4198.

(13) Rogge, S. M. J.; Bavykina, A.; Hajek, J.; Garcia, H.; Olivares-Suarez, A. I.; Sepulveda-Escribano, A.; Vimont, A.; Clet, G.; Bazin, P.; Kapteijn, F.; Daturi, M.; Ramos-Fernandez, E. V.; Llabres i Xamena, F. X.; Van Speybroeck, V.; Gascon, J. Metal–organic and covalent organic frameworks as single-site catalysts. *Chem. Soc. Rev.* **2017**, *46*, 3134–3184.

(14) Sheldrick, G. M. *SHELXS-2014, Program for the Solution and Refinement of Crystal Structures*; University of Göttingen: Göttingen, Germany, 2014.

(15) Spek, A. L. *PLATON, a Multipurpose Crystallographic Tool*; Utrecht University: Utrecht, The Netherlands, 1998.

(16) Blatov, V. A.; Carlucci, L.; Ciani, G.; Proserpio, D. M. Interpenetrating metal–organic and inorganic 3D networks: a computer-aided systematic investigation. Part I. Analysis of the Cambridge structural database. *CrystEngComm* **2004**, *6*, 377–395.

(17) KAPPE, C. O. Acc. Recent Advances in the Biginelli Dihydropyrimidine Synthesis. New Tricks from an Old Dog. *Acc. Chem. Res.* **2000**, *33*, 879–888.

(18) Saikia, M.; Bhuyan, D.; Saikia, L. Keggin type phosphotungstic acid encapsulated chromium (III)terephthalate metal organic framework as active catalyst for Biginelli condensation. *Appl. Catal., A* **2015**, *505*, 501–506.

(19) Pal, T. K.; De, D.; Senthilkumar, S.; Neogi, S.; Bharadwaj, P. K. A Partially Fluorinated, Water-Stable Cu(II)–MOF Derived via Transmetalation: Significant Gas Adsorption with High CO₂ Selectivity and Catalysis of Biginelli Reactions. *Inorg. Chem.* **2016**, *55*, 7835–7842.

(20) Rostamnia, S.; Morsali, A. Basic isoreticular nanoporous metal–organic framework for Biginelli and Hantzsch coupling: IR-MOF-3 as a green and recoverable heterogeneous catalyst in solvent-free conditions. *RSC Adv.* **2014**, *4*, 10514–10518.

(21) Verma, A.; De, D.; Tomar, K.; Bharadwaj, P. K. An Amine Functionalized Metal–Organic Framework as an Effective Catalyst for Conversion of CO₂ and Biginelli Reactions. *Inorg. Chem.* **2017**, *56*, 9765–9771.

(22) Wang, J. H.; Tang, G. M.; Wang, Y. T.; Cui, Y. Z.; Wang, J. J.; Ng, S. W. A series of phenyl sulfonate metal coordination polymers as catalysts for one-pot Biginelli reaction under solvent free conditions. *Dalton Trans* **2015**, *44*, 17829–17840.

(23) Kumar, A.; Maurya, R. A. Synthesis of 3,4-dihydropyrimidin-2(1H)-ones using Ziegler–Natta catalyst system under solvent free conditions. *J. Mol. Catal. A: Chem.* **2007**, *272*, 53–56.

(24) Emeis, C. A. Determination of Integrated Molar Extinction Coefficients of Infrared Absorption Bands of Pyridine Adsorbed on Solid Acid Catalysts. *J. Catal.* **1993**, *141*, 347–354.